Biophysical Aspects of Auger Processes, AAPM Symposium Series No. 8 (1992) 137-152
Eds. RW Howell, VR Narra, KSR Sastry, DV Rao

SIMULATION OF STRAND BREAK INDUCTION BY DNA INCORPORATED ^{125}I

EKKEHARD POMPLUN[1], MARTINE ROCH[2], and MICHEL TERRISSOL[2]

[1]Abteilung Sicherheit und Strahlenschutz, Forschungszentrum Jülich GmbH, Postfach 1913, 5170 Jülich, Germany

[2]Centre de Physique Atomique, Universite Paul Sabatier, 118 route de Narbonne, 31062 Toulouse Cedex, France

ABSTRACT

Monte Carlo calculation of ^{125}I Auger cascades has provided electron spectra for individual decays with kinetic energies determined by Dirac-Fock methods. For these Auger electrons, track structures in liquid water have been generated and superimposed on a straight DNA plasmid model with atomic coordinates taken from X ray diffraction studies. Due to its high geometrical resolution, this DNA model makes it possible to localize the energy deposition or/and radical production events relative to the sub-molecular units of the DNA strands (base, sugar, phosphate). Furthermore, it is possible to distinguish between events inside (direct) and outside (indirect, radical production) of the atomic volumes of the DNA. On the basis of different assumptions for the effectiveness of strand break induction by direct hits and by OH· and H· radicals, the yields for single- and double strand breaks, as well as the strand break distribution as a function of the distance from the decay site, has been evaluated and compared with experimental and theoretical results from the literature.

INTRODUCTION

It is well known that Monte Carlo simulation represents a very good way of investigation for the understanding of radiation damage at the molecular level. A source of radiation which induces a specific pattern of damage within a distance of a few molecules only can be seen with DNA-incorporated Auger electron emitters, *e.g.* ^{125}I. This nuclide has been demonstrated to possess high-LET-like biological effectiveness when it is incorporated in the DNA molecule. A decay site only a few nanometers apart from this critical target will drastically reduce its efficiency (1). Due to this particular character of damage, the Auger electrons released by ^{125}I represent a most useful tool in radiation biology. The Monte Carlo codes that simulate the electron spectra of individual decays (2,3) and that generate track structures (4,5), in combination with superimposing the tracks on an atomic DNA target model (6), are expected to provide information about the radiation action mechanism.

Since the details of these mechanisms are still unknown, one has to introduce different assumptions for the relationship between energy deposition events and the resulting biological effects in order to simulate the radiation damage. To validate these assumptions, a comparison with experimental results is necessary. A pioneering experiment for the determination of the spatial distribution of biological damage on the DNA scale was performed by Martin and Haseltine (7). These authors labeled a linear segment of plasmid DNA with ^{32}P at a position 58 base pairs away from the site of a decaying ^{125}I nuclide. By measuring the length of the phosphorus-labeled DNA-fragments, a distribution of those strand breaks could be derived which are most distant from the ^{125}I position.

Charlton and Humm (8) made use of this experimental data when they introduced a method to calculate the number of DNA strand breaks. They generated water vapor track structures for the ^{125}I Auger electrons and compared these tracks with a geometrical DNA model. This model is described by a straight cylinder consisting of three parts, an inner core representing the base pairs, and around this core semi-annuli representing the phosphate/sugar chain. All the energy transfer events taking place inside the phosphate/sugar volumes were counted to be effective in terms of strand break induction when the amount of energy deposited was above a certain threshold (17.5 eV). Without any further assumptions the authors found a surprisingly good coincidence with the experimental results of Martin and

Haseltine (7). In another recent paper, Pomplun (6) assessed by principally the same technique the energy deposition in and near the different submolecules of the DNA and estimated the number of strand breaks caused by direct and indirect effects. The target model used allowed a geometric atomic scale resolution based on the coordinates of the individual DNA atoms (9,10). In particular, the importance of those Auger electrons with a kinetic energy of $E \leq 500$ eV could be revealed, thereby demonstrating the necessity to determine these energies as accurate as possible. The calculation of the Auger electron kinetic energies by the empirical (Z+1)-approximation, normally sufficient in the case of single charged atoms, leads to a more or less strong energy imbalance when applied for cascade released electrons (11).

Another important aspect of these two papers must be seen in the application of water vapor track structures which may induce significant uncertainties in the localization of energy deposition events with regard to the nanometer scale of the DNA target models. There are two main reasons to use liquid water conditions for the particle transport code rather than those for water vapor: 1) The production of secondary electrons is not always localized at the site of initial energy transfer (12,13). In liquid water, inelastic collisions may involve thousands, even 10^6 or more electrons, and the collective excitations can produce H_2O^+ or H_2O^* at sites situated up to several nanometers from the primary trajectory. It is the reason we use liquid water cross-sections derived from dielectric theory in which liquid water is assumed to respond to the passage of charged particles as any dielectric medium responds to an electromagnetic disturbance (12). 2) The physico-chemical step (10^{-15} s to 10^{-12} s) must not be neglected. During this step subexcitation electrons may recombine and/or thermalize, early physico-chemical events arise and then the chemical stage begins with diffusion and chemical reactions of all species created: e^-_{aq}, $OH\cdot$, $H\cdot$, H_3O^+, H_2O_2, OH^-, H_2, HO_2. Furthermore, the liquid water code identifies the chemical species created by the energy deposition events of the tracks. This opens the possibility to trace individual radicals or *e.g.* to exclude all those species from further consideration which are supposed not to react efficiently with the DNA (see METHODS).

In this paper we try to utilize these advantages in the simulation of strand break induction by DNA incorporated ^{125}I on the basis of liquid water track structures. To have accurate Auger electron kinetic energies, the initial electron spectrum was calculated with a Dirac-Fock approach (3). By introducing specific assumptions for the damaging effectiveness of individual

chemical species, the numbers of SSB and DSB as well as the local distribution of the breaks will be evaluated and compared with experimental results. The fractions of direct and indirect hit modes contributing to the total number of breaks will also be given.

METHODS

The Auger electron spectrum of ^{125}I has been generated by Monte Carlo simulation of the Auger cascades produced by electron capture which is the first step in the decay of ^{125}I. To determine the electron kinetic energy the difference between the total energy of the (multiple) ionized atom before and after the Auger electron emission was calculated. For details see Ref. (3).

For track structure generation we used three Monte Carlo type codes chained together as described in Ref. (26) to obtain the space and time evolution of each chemical species created during the slowing-down of electrons in liquid water. Input data for the physical step (up to 10^{-15} s) are cross-sections derived from the dielectric response function (13) from electron scattering in gases (14) or theory. During the physico-chemical step (10^{-15} s to 10^{-12} s), the subexcitation electrons are transported with the use of cross-sections measured in amorphous ice (15,16), while recombination and thermalization follow the Onsager-Debye theories, and dissociation semi-empirical ones. Finally, in the chemical step (10^{-12} s to seconds), about twenty-five reactions are considered and species diffuse according to the Smoluchowski law.

The DNA target model used here (see Fig. 1) has been described in detail elsewhere (6). It is based on the geometric coordinates of the individual DNA atoms allowing a very high geometric resolution. Only those energy deposition events were considered which take place inside a volume of interest represented by a virtual cylinder enveloping all nucleotides of the straight DNA segment. This includes also the structural water molecules in the major and minor grooves for which individual coordinates are not available. Due to the lack in knowledge of the species and radicals created by electron-DNA direct interactions, we have only used the chemical species from the physical stage in this third part of this study, and it has been assumed that no radical from the environmental regions will diffuse into this volume of interest nor any radical will escape from this volume. Such a situation reflects a frozen state condition. Therefore, the numbers of SSB and

DSB calculated here have been compared with the experimentally derived data reported by LeMotte and Little (17) for human cells at -90°C.

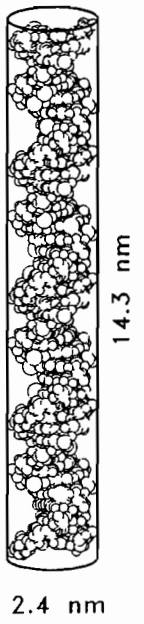

FIG. 1. DNA target model (inclined by 15°); the ^{125}I is positioned at the site of the methyl group of the 41st base (out of 82) which has been assumed here to be thymine. This position is 0.56 nm distant from the central helix axis. The volume of interest is indicated by the virtual cylinder.

The strand break induction has been simulated here in the following way: all the energy deposition events located inside the van der Waals radius of a phosphate-group or sugar atom were counted as SSB caused by direct hits if the amount of deposited energy in the phosphate/sugar molecule was greater than a threshold value of 18 eV (see next chapter). For the indirect effects from all the radicals evaluated by the track structure code, only the primary water radicals OH·, H· and e^-_{aq} have been assumed here to react with the DNA (see *e.g.* Refs. 18,19). However, e^-_{aq} was neglected for strand

break induction due to the studies of Lemaire *et al.* (20) for poly U and of Nabben *et al.* (21) for the inactivation of double-stranded DNA, whereas the effectiveness of OH· and H· were supposed to be equal (21). As possible mechanisms for strand break induction by the OH· radicals the hydrogen abstraction from deoxyribose and the hydroxyl addition to bases are discussed (22), the H· radical is supposed to act also via base radicals (20). All other radicals have been excluded from further consideration. Two SSB on opposite strands within a distance of less than 20 base pairs have been detected as one DSB (for a more detailed discussion see Ref. 6). For the simulation of the Martin and Haseltine (7) experiment only those strand breaks have been considered which - according to the experimental design - are furthest from ^{125}I.

RESULTS AND DISCUSSION

For all particles belonging to each ^{125}I decay, a data set in a four coordinate system (t, x, y, z) is obtained for each species: e^-_{aq}, OH·, H·, H_3O^+, H_2O_2, OH^-, H_2, HO_2 between 10^{-15} s and 1 second. In Fig. 2 (a-d) are represented three-D space and time evolutions (all species together) for one randomly chosen ^{125}I decay in liquid water. Figs. 3 and 4 are zooms near the initial ^{125}I decay point, assumed at axes origin. On all axes, the distance unit is nanometers. No interaction with any atom from the target model has been considered here.

In Fig. 5 we have plotted the average number of chemical species produced in 10^{-12} s in spherical shells of thickness one nanometer centered at the site of ^{125}I decay. The shapes for OH·, H· and H_3O^+ species are very close to the initial (10^{-15} s) dose point kernel obtained for ^{125}I decays. The hydrated electron smooth curve is due to the recombination, diffusion and thermalization of subexcitation electrons created at 10^{-15} s with energies up to 7.4 eV. If we compare this result with same found in literature (23), the shapes are very similar except for hydrated electrons and absolute values. There are two reasons for the discrepancies: first, the absolute number of species per decay is strongly dependent on the ^{125}I cascade electron spectra. Secondly, for hydrated electrons, the travel distance depends on elastic and inelastic cross-sections, diffusion coefficient and the recombination model used between 10^{-15} s and 10^{-12} s, the physico-chemical step.

a

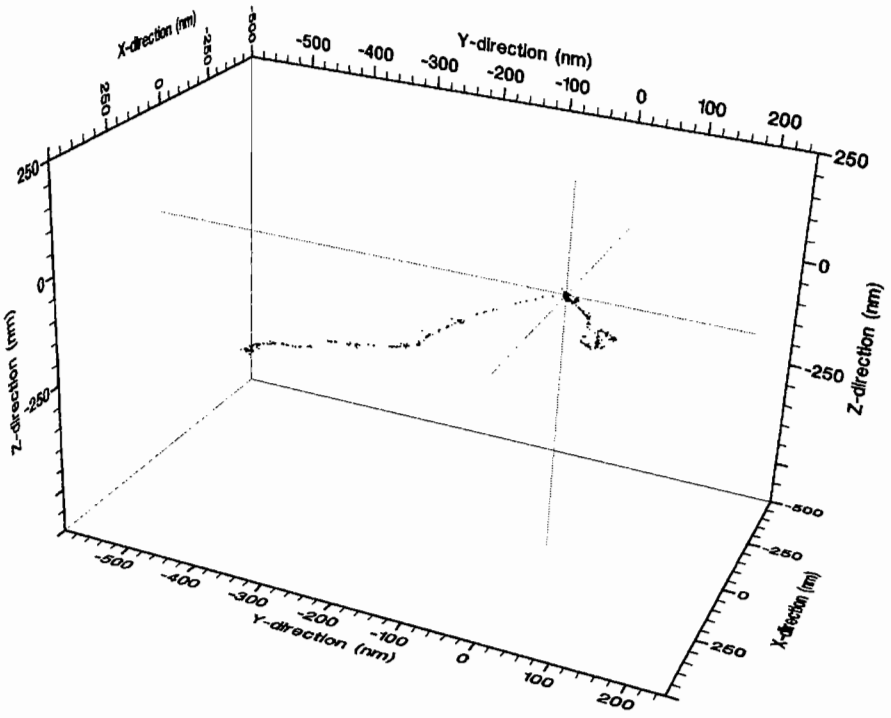
X-direction (nm)
Y-direction (nm)
Z-direction (nm)
Z-direction (nm)
X-direction (nm)
Y-direction (nm)

b

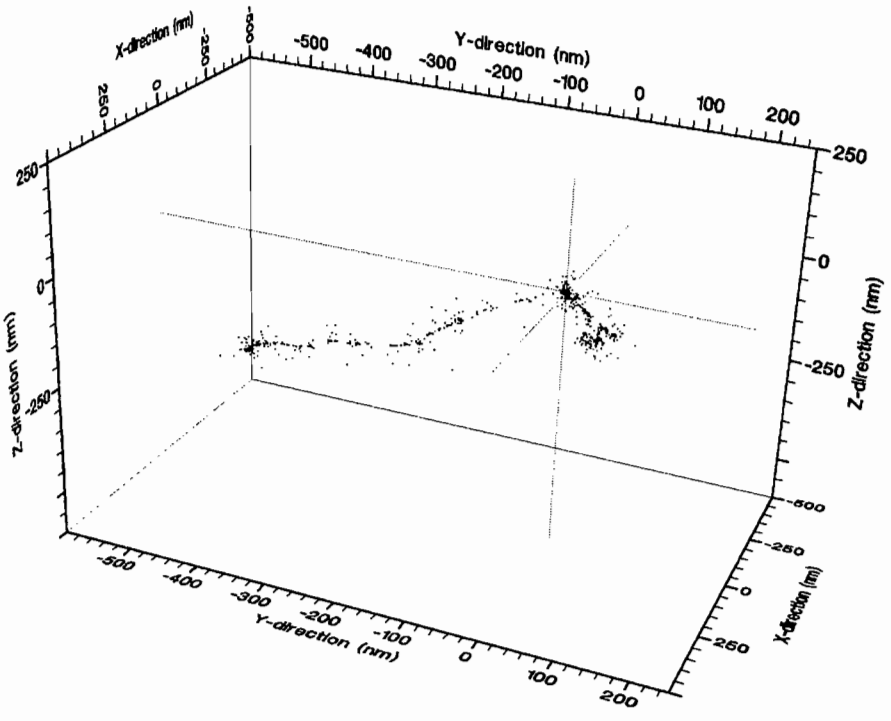
X-direction (nm)
Y-direction (nm)
Z-direction (nm)
Z-direction (nm)
X-direction (nm)
Y-direction (nm)

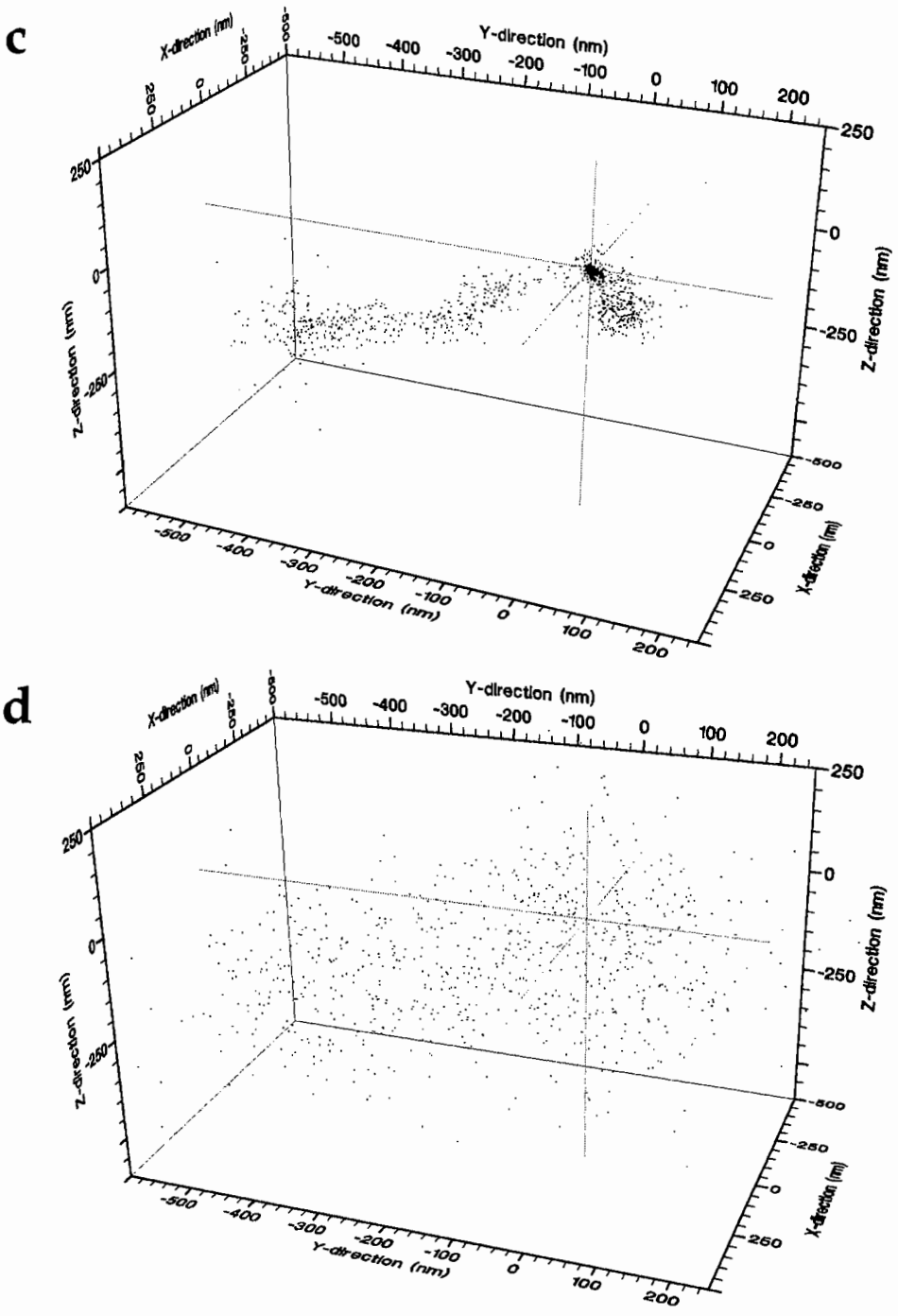

FIG. 2. Complete track of one randomly chosen ^{125}I-decay for (a) 10^{-15} s, (b) 10^{-12} s, (c) 10^{-9} s, (d) 10^{-8} s.

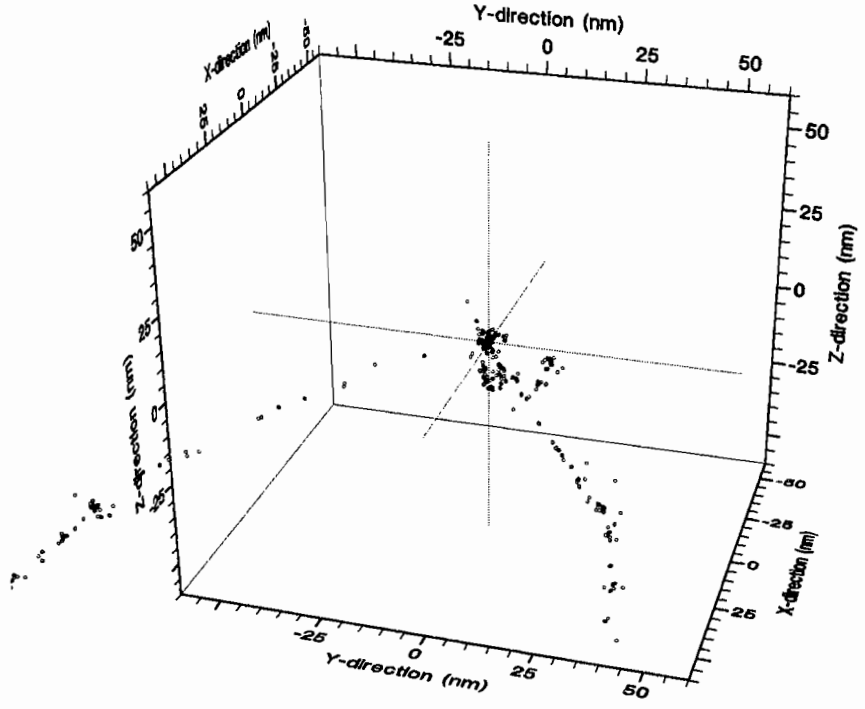

FIG. 3. Zoom from Fig. 2a.

The best agreement with the experimental data of Martin and Haseltine (7) for the spatial distribution of those strand breaks furthest from ^{125}I were obtained by using a threshold energy of 18 eV for direct hits. Charlton and Humm (8) found nearly the same value (17.5 eV). Until now only the labeled strand could be considered (Fig. 6) demonstrating that in the immediate vicinity of the decay site - where the overwhelming number of breaks have been found experimentally - the calculated values fit very well. For comparison the water vapor tracks generated by the MOCA8 code (4) for the same electron spectrum have been used to simulate the Martin and Haseltine (7) experiment. In this case, energy deposition events of $E > 18$ eV inside an atom of the phosphate/sugar group (direct hit) or near to these submolecules (indirect hits) were assumed to be effective in strand break induction. The results of this simulation are shown in Fig. 6. Whereas for distances of three and more base pairs from the decay site there are only small differences between the liquid water and the water vapor data. The latter ones

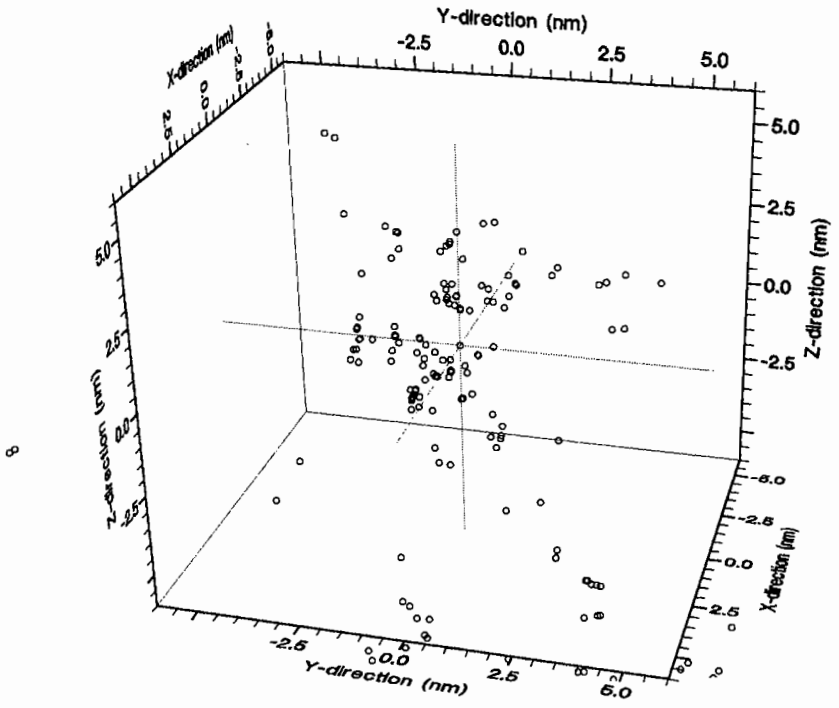

FIG. 4. Zoom from Fig. 2a.

significantly disagree with the experimental distribution by revealing less breaks at the site of decay and too many at distances of one and two base pairs apart from the labeled base. Due to the satisfactory results obtained by the liquid water tracks, the contribution of each of the two hit modes has been assessed. As can be seen from Fig. 7, the characteristic shape of the curve for all hits (taken from Fig. 6) is determined by the direct hit pattern in the region from '0' to '5' base pairs distance. The number of radical-induced breaks (indirect hits) falls more or less continuously with a steep decline (parallel to the direct hits) between the second and third base pair from the site of decay. It should be noted here that there is an inherent bias in these curves due to the experimental condition of measuring the farthest breaks only; additional breaks at positions nearer to the decaying ^{125}I are masked.

The results for the total numbers of strand breaks per ^{125}I decay are summarized in Table I. The water vapor values additionally shown here were obtained by recalculation of data from Ref. (6) by increasing the

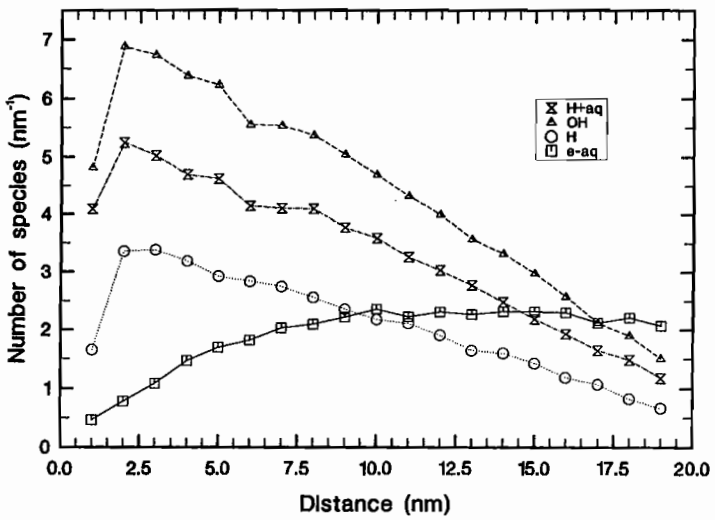

FIG. 5. Number of different species inside spherical shells around the decay.

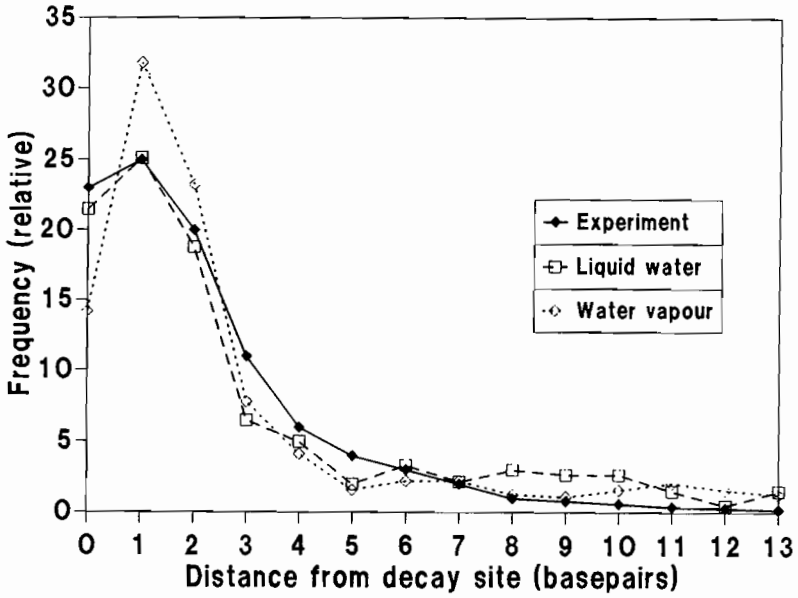

FIG. 6. Spatial distribution of ^{125}I induced DNA strand breaks; comparison of liquid water and water vapor calculations with experimental results from Martin and Haseltine (7).

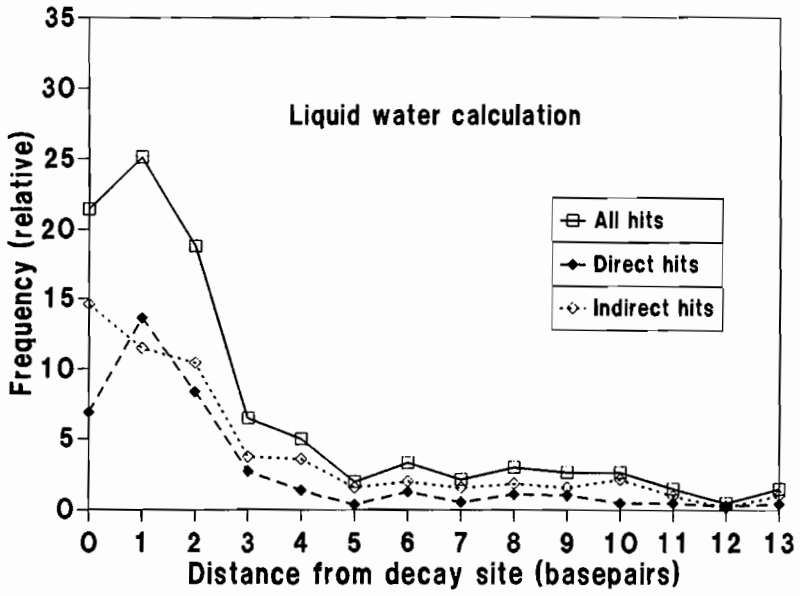

FIG. 7. Calculated direct and indirect hit mode fractions in the distribution of DNA strand breaks for liquid water conditions.

TABLE I
Number of SSB and DSB per ^{125}I Decay

Kind of Break	DNA-Helix Model		Experiment
	Liquid Water	Water Vapor	Human Diploid cells -90°C
SSB (total)	2.9	2.9	3.0 (4.3±1.2)
SSB (corr.)	1.7	1.6	1.7 (2.4)
DSB	0.6	0.7	0.6 (0.86±0.3)

Due to the best fit values obtained in this work (energy threshold for direct hits E > 18 eV) the values published in Ref. (6) have been recalculated using this threshold instead of E > 10 eV, the original experimental results from Ref. (17) (in brackets) have been reduced by 30% due to the alkaline elution technique (see Ref. (25)).

threshold values for direct hits (see above) from 10 eV to 18 eV. For indirect hits a threshold of 17 eV was taken according to Chatterjee and Magee (24). For the comparability of the experimental conditions with the data calculated here see Ref. (6). Due to the alkali elution technique used by LeMotte and Little (17), these values have been reduced by 30% (25). On first view it might be surprising that considerably less than 1 DSB per decay - the expected value from many studies - is found here. However, in the frozen state situation simulated here, the radicals will become relatively immobile so that only those species produced in the water sheaths of the DNA may react efficiently. On the other hand, possible repair processes are suppressed at these temperatures. With regard to the number of breaks both of these effects (immobilization of radicals outside the volume of interest and inhibition of repair) would have opposite directions (with an unknown net effect) but for this high-LET Auger electron radiation it seems to be reasonable to expect for room temperature conditions a stronger influence of the radicals than of the repair so that by the elimination of both effects due to frozen state the number of breaks should be lower than under room temperature. In general, there is a good agreement between all three sets of data without any significant difference between the water vapor and the liquid water data. The advantage, however, which can be taken from the liquid water data is given by the more detailed information about the involved radiation action mechanisms which had been incorporated into the DNAMOD code (6) controlling the interaction of the tracks with the target model. In particular only OH· and H· radicals attacking the sugar and bases are responsible for strand breaks by indirect effects (see METHODS).

This sophisticated model (^{125}I decay + track generation + DNA model) will be a very useful tool when more precise electron-DNA cross-sections and physico-chemical data on the electron diffusion and reactions with water species are known.

CONCLUSIONS

Track structures of Auger electrons released by ^{125}I decay have been generated for liquid water conditions. By superimposing these tracks onto a DNA target model, the strand break induction by direct hits as well as by radical attack were simulated. A satisfactory agreement with experimentally determined spatial distribution of the breaks could be achieved by introducing an energy threshold of $E > 18$ eV for direct hits and by considering only OH·

and H· radicals out of all the chemical species. Whereas about two thirds of the strand breaks at the site of decay (labeled nucleotide) seem to be induced by radical attack, the direct hits by Auger electrons are responsible for the peak in the distribution at the neighboring nucleotide position (Fig. 7). The total number of SSB and DSB calculated here also agree very well with experimental findings. These results support radical-behavior mechanisms suggested in the literature.

REFERENCES

1. D.E. CHARLTON, The range of high-LET effects from ^{125}I decays. *Radiat. Res.* **107**, 163-171 (1986).
2. D.E. CHARLTON and J. BOOZ, A Monte Carlo treatment of the decay of ^{125}I. *Radiat. Res.* **87**, 10-23 (1981).
3. E. POMPLUN, J. BOOZ, and D.E. CHARLTON, A Monte Carlo simulation of Auger cascades. *Radiat. Res.* **111**, 533-552 (1987).
4. H.G. PARETZKE, Radiation track structure theory. In *Kinetics of Nonhomogeneous Processes*, (G.R. FREEMAN, Ed.), Wiley, New York, pp. 89-170, 1987.
5. M. TERRISSOL and A. BEAUDRE, Simulation of space and time evolution of radiolytic species induced by electrons in water. *Radiat. Prot. Dosim.* **31**, 171-175 (1990).
6. E. POMPLUN, A new DNA target model for track structure calculations and its first application to I-125 Auger electrons. *Int. J. Radiat. Biol.* **59**, 625-642 (1991).
7. R.F. MARTIN and W.A. HASELTINE, Range of radiochemical damage to DNA with decay of iodine-125. *Science*, **213**, 896-898 (1981).
8. D.E. CHARLTON and J.L. HUMM, A method of calculating initial DNA strand breakage following the decay of incorporated ^{125}I. *Int. J. Radiat. Biol.* **53**, 353-365 (1988).
9. S. ARNOTT and D.W.L. HUKINS, Refinement of the structure of B-DNA and implications for the analysis of X ray diffraction data from fibers of biopolymers. *J. Mol. Biol.* **81**, 93-105 (1973).
10. R. CHANDRASEKARAN and S. ARNOTT, *The structures of DNA and RNA helices in oriented fibers*. Landolt-Börnstein, New Series VII, 1b, Springer-Verlag, Berlin, 1989.
11. E. POMPLUN, ^{123}I: Calculation of the Auger electron spectrum and assessment of the strand breakage efficiency. (this volume).
12. R.H. RITCHIE, R.N. HAMM, J.E. TURNER, and H.A. WRIGHT, The interaction of swift electrons with liquid water. In *Proceedings of the Sixth Symposium on Microdosimetry*, Brussels, Belgium, EUR 6064, London: Harwood Academic, pp. 345-354, 1978.
13. J.M. HELLER, R.N. HAMM, R.D. BIRKHOFF, and L.R. PAINTER, Collective oscillation in liquid water. *J. Chem. Phys.*. **60**, 3483-3486 (1974).
14. G.J. KUTCHER and A.E.S. GREEN, A model for energy deposition in liquid water. *Radiat. Res.* **67**, 408-425 (1976).
15. M. MICHAUD and L. SANCHE, Total cross-section for slow electron (1-20 eV) scattering in solid H_2O. *Phys. Rev.* **A36**, 4672-4683 (1987).
16. M. MICHAUD and L. SANCHE, Absolute vibrational excitation cross-sections for slow electron (1-18 eV) scattering in solid H_2O. *Phys. Rev.* **A36**, 4684-4699 (1987).
17. P.K. LEMOTTE and J.B. LITTLE, DNA damage induced in human diploid cells by decay of incorporated radionuclides. *Cancer Res.* **44**, 1337-1342 (1984).

18. D. SCHULTE-FROHLINDE, Comparison of mechanisms for DNA strand break formation by the direct and indirect effect of radiation, In *Mechanisms of DNA damage and repair*, (G.M. SIMIC *et al.*, Eds.) pp. 19-27, Plenum Press, New York, 1986.
19. M.V.M. LAFLEUR and H. LOMAN, Radiation damage to ϕX174 DNA and biological effects. *Radiat. Environ. Biophys.* **25**, 159-173 (1986).
20. D.G.E. LEMAIRE, E. BOTHE, and D. SCHULTE-FROHLINDE, Yields of radiation-induced main chain scission of poly U in aqueous solution: strand break formation via base radicals. *Int. J. Radiat. Biol.* **45**, 351-358 (1984).
21. F.J. NABBEN, M.V.M. LAFLEUR, J.C.M. SIKKERS, A.C. LOMAN, J. RETEL, and H. LOMAN, Repair of damage in double-stranded ϕX174 (RF) DNA due to radiation-induced water radicals. *Int. J. Radiat. Biol.* **45**, 379-388 (1984).
22. D. SCHULTE-FROHLINDE, Mechanisms of strand breaks in DNA induced by OH radicals in aqueous solution. In *Proc. 6th Int. Congr. Radiat. Res.* (S. OKADA *et al.*, Eds.), pp. 407-422, Mazuren, Tokyo, 1979.
23. H.A. WRIGHT, R.N. HAMM, J.E. TURNER, R.W. HOWELL, D.V. RAO, and K.S.R. SASTRY, Calculation of physical and chemical reactions with DNA in aqueous solution from Auger cascades. *Radiat. Prot. Dosim.* **31**, 59-62 (1990).
24. A. CHATTERJEE and J.L. MAGEE, Theoretical investigation of the production of strand breaks in DNA by water radicals. *Radiat. Prot. Dosim.* **13**, 137-140 (1985).
25. R. ROOTS, G. KRAFT, and E. GOSSCHALK, The formation of radiation-induced DNA breaks: the ratio of double-strand breaks to single-strand breaks. *Int. J. Radiat. Oncol. Biol. Phys.* **11**, 259-265 (1985).
26. A. BEAUDRE, Simulation spatio-temporelle des processus radiolytiques induits dans l'eau par des électrons. Thèse de l'Université Paul Sabatier, Toulouse, France, No. 371, 1988.

DISCUSSION

Hofer, K. G. According to early work by Burki, the oxygen effect for ^{125}I damage is quite small. Here you claim that indirect effects are quite prominent. How do you reconcile this apparent discrepancy?

Pomplun, E. The approach used here considers only the DNA itself, including the structural water in the grooves, so that the terms direct and indirect effects also refer to this volume only. Effects like the oxygen effect which depend on the conditions in the environment of the DNA are not taken into account here. In this sense, the calculations simulate a frozen state situation with an assumed immobilization of radicals. Only those radicals which are produced in the nearest surroundings of the DNA molecule, namely inside the 2.4 nm diameter cylinder, are expected here to attack the DNA strands.

Nikjoo, J. We need to move from the concepts of direct and indirect effect to mechanisms of SSB production.

Pomplun, E. By the classical terms direct effects and indirect effects, a clear distinction between two different mechanisms is made. As long as no more precise mechanisms are fully understood, I think we should retain these terms.

Humm, J. L. You showed (6) that 90% of the strand break contributing energy deposition arises from electrons of energies < 500 eV (*i.e.* M & N

Auger and Coster-Kronig electrons). Accurate DNA dose specification therefore depends on the accurate evaluation of these electrons. The current Auger electron Monte Carlo calculations agree on the K and L Auger series, but deviations become more significant for the lowest energy electrons. You showed differences of nearly a factor of two in the low energy electron yields and energies for the different methods. Yet the DNA strand break yields you showed using your Auger cascade code and the simpler code of Charlton & Booz were in close agreement. Do you think that this is due to the enormous magnitude of ^{125}I decay, making it an unsuitable isotope as the basis for different Monte Carlo simulation code comparison? Perhaps such comparisons should be made with an isotope emitting a small number of Auger electrons such as ^{55}Fe. Do you agree?

Pomplun, E. Both strand break calculations have been performed not only with different electron spectra but also with different DNA models and, what could be of special importance, different ^{125}I positions relative to the central DNA axis. Therefore, it would be very interesting, first, to repeat the calculations for both electron spectra on the basis of equal models and ^{125}I positions. If the close agreement in the strand break remains, the enormous magnitude of ^{125}I decay could be an explanation for masking differences in the electron spectra. In that case one should indeed use an isotope like ^{55}Fe to demonstrate the differences in the electron spectra as being responsible for differences in strand break yields.